Development 122, 3229-3242 (1996)
Printed in Great Britain © The Company of Biologists Limited 1996
DEV2076

Rhombencephalic neural crest segmentation is preserved throughout craniofacial ontogeny

Georgy Köntges and Andrew Lumsden

MRC Brain Development Programme, Department of Developmental Neurobiology, UMDS, Guy's Hospital, London SE1 9RT, UK

SUMMARY

To investigate the influence of hindbrain segmentation on craniofacial patterning we have studied the long term fate of neural crest (NC) subpopulations of individual rhombomeres (r), using quail-chick chimeras. Mapping of all skeletal and muscle connective tissues developing from these small regions revealed several novel features of the cranial neural crest. First, the mandibular arch skeleton has a composite origin in which the proximal elements are r1+r2 derived, whereas more distal ones are exclusively midbrain derived. The most proximal region of the lower jaw is derived from second arch (r4) NC. Second, both the lower jaw and tongue skeleton display an organisation which precisely reflects the rostrocaudal order of segmental crest deployment from the embryonic hindbrain. Third, cryptic intraskeletal boundaries, which do not correspond to anatomical landmarks, form sharply defined interfaces between r1+r2, r4 and r6+r7 crest. Cells that survive the early apoptotic elimination of premigratory NC in r3 and r5 are restricted to tiny contributions within the 2nd arch (r4) skeleton. Fourth, a highly constrained pattern of cranial skeletomuscular connectivity was found that precisely respects the positional origin of its constitutive crest: each rhombomeric population remains coherent throughout ontogeny, forming both the connective tissues of specific muscles and their respective attachment sites onto the neuro- and viscerocranium. Finally, focal clusters of crest cells, confined to the attachment sites of branchial muscles, intrude into the otherwise mesodermal cranial base. In the viscerocranium, an equally strict, rhombomere-specific matching of muscle connective tissues and their attachment sites is found for all branchial and tongue (hypoglossal) muscles. This coherence of segmental crest populations explains how cranial skeletomuscular pattern can be implemented and conserved despite evolutionary changes in the shapes of skeletal elements.

Key words: connective tissues, muscle patterning, fate mapping, chick-quail chimeras, rhombomeres, neural crest, segmentation, vertebrate head, evolution

INTRODUCTION

Patterning tasks for a developing vertebrate head include the definition of skeletal and muscular shapes and the establishment of a precise network of skeletomuscular connections. It has long been suspected that cranial neural crest (NC), a novel feature of craniates (Gans and Northcutt, 1983), might play an important role in these two aspects of head patterning. Regional fate maps have already revealed the extensive contribution of cranial NC versus mesoderm (Couly et al., 1993; Le Lièvre and Le Douarin, 1975; Le Lièvre, 1978; Noden, 1983b, 1988), but its specific role in patterning has remained elusive.

The idea that regional diversity in the head emerges from early differences in the morphogenetic specification of individual NC populations was deduced from hetero- and isotopic grafting experiments in amphibian (Hörstadius and Sellman, 1946; Wagner, 1949) and avian (Noden, 1983a) embryos. But these experimental results have remained controversial because no premigratory NC subpopulations other than the mandibular one seems to be specified with respect to subsequent pattern. Furthermore, even mandibular crest does not produce a complete set of (mandibular) skeletal derivatives when grafted heterotopically.

In previous cranial NC transplantation studies, no reference was made to natural landmarks along the neuraxis and a possible developmental relationship between cranial NC and CNS patterns was not considered. New light has been shed on this possibility by the new appreciation that the embryonic hindbrain, a prominent source of NC, is a segmented structure (Lumsden and Keynes, 1989) and, furthermore, that NC deployment from this region is, in contrast to the rest of the neuraxis, discontinuous (Fig. 1A). Thus, the first arch (mandibular) is populated by NC from midbrain, rhombomere (r) 1 and r2 (Fig. 1A,D,F), the second arch (hyoid) is populated by r4 NC (Fig. 1A,G) and the third arch by NC from r6 and r7 (Lumsden et al., 1991). These subpopulations of cranial NC form discrete (i.e. non-mixing) streams as they migrate into their respective arches, a segregation that may relate directly to the fact that there are gaps in NC production corresponding to r3 and r5 (Lumsden et al., 1991; Graham et al., 1993). The selective elimination of premigratory NC from r3 and r5 involves signalling interactions between even- and odd-numbered rhombomeres (Graham et al., 1994). The extent and significance of this patterned apoptotic NC depletion, however, became controversial when another vital dye labelling study using fluorescence videomicroscopy (Birgbauer et al., 1995)

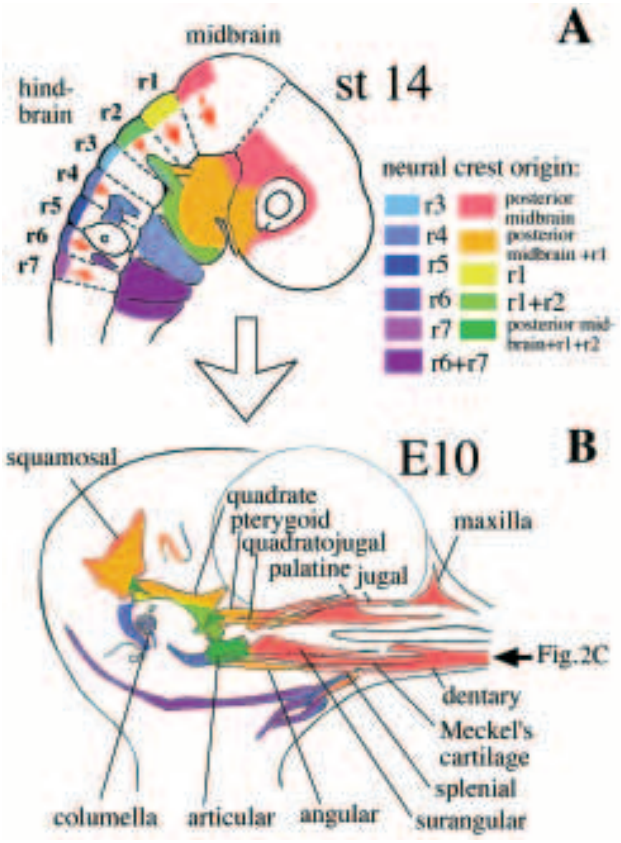

Fig. 1. Embryonic origin and fate of individual cranial neural crest subpopulations in the chick embryo at st 14 (A) and E10 (B). A is modified after Lumsden et al. (1991). The otic and tongue regions are detailed in Figs 2A, 4. (C-G) Relative rhombomeric origin and localisation of quail neural crest cells is identical to that reported by Lumsden et al. (1991) for chick NC, using DiI. As in all other photographs quail cells as detected by the Q¢PN antibody, are HRP-labelled and dark brown. (C) Dorsal view of st 19 chimeric hindbrain, r1 being isotopically replaced by quail r1 at st 8+. Compare with E for accuracy of r1/r2 grafting at st 8+/9–. (D) Lateral view of same embryo showing quail NC cells in the trigeminal exit point (asterisk adjacent to r2), the trigeminal nerve, mandibular and maxillary process of branchial arch 1 (b1) and behind the eye (cf. Lumsden et al., 1991). No NC cells are found in other branchial arches (b2). (E) Dorsal view of st. 15 chimeric hindbrain, r2 was replaced by quail r2 at st 9–. (F) Lateral view of same embryo showing quail r2-NC cells restricted (arrows) to the mandibular process of the 1st arch (b1) (cf. Lumsden et al., 1991). No cells are found in the 2nd branchial arch (b2). (G) Lateral view of a st. 15 chimera with r4 being replaced by quail r4 at st. 9. The 2nd branchial arch (hyoid, b2) is entirely filled by postmigratory quail crest cells from r4 which do not migrate to any other branchial arch (cf. Lumsden et al., 1991). Some crest cells in the roofplate of the hindbrain migrate posteriorly, but do not enter other branchial arches (b1,3,4).

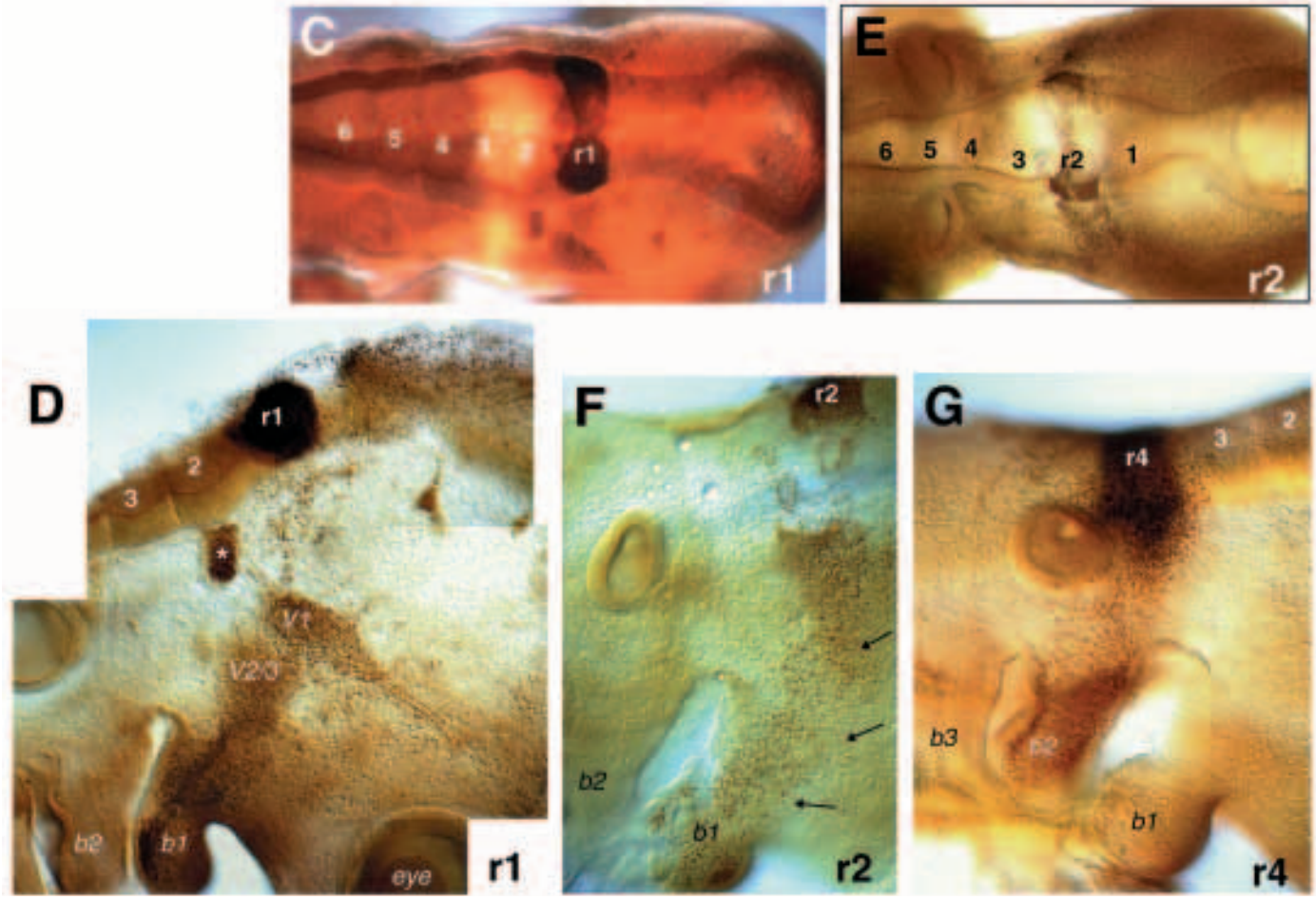

revealed a peculiar behavior of the surviving NC cells in r3 and r5: the NC progenitor region appears to spread in a rostrocaudal direction such that cells originating in r3 and r5 escape apoptosis and exit the neural tube at the axial levels of r2, 4 and 6. This observation seemed to counter the notion that positional values on the rostrocaudal axis of the hindbrain (and therefore also within its emanating NC populations) are already fixed at the stage of NC emigration.

We wanted to assess the impact of hindbrain segmentation on craniofacial patterning and, specifically the significance of r3 and r5 NC cell depletion; for these purposes it was necessary to fate map each rhombomeric NC subpopulation - using the quail marker (Le Douarin, 1969) to allow long-term detection. Earlier studies on NC have focused almost exclusively on how the shapes of visceroskeletal elements are defined. The other, equally important facet of head patterning, the establishment of skeletomuscular connectivity, however, has received little attention. We have, therefore, scanned chimeric heads for quail cells in all skeletal as well as muscle connective tissue derivatives. The resulting rhombomeric NC fate map provides a complete set of morphological criteria for estimating morphogenetic specification of each rhombomeric NC subpopulation. Furthermore, it defines the embryological framework for a more refined interpretation of functional studies involving two homeobox-containing genes, *Hoxa-2* and *Otx-2*. Their null mutation results in distinct and highly specific craniofacial phenotypes (Rijli et al., 1993; Gendron-Maguire et al., 1993; Matsuo et al., 1995).

We find that most elements of the visceral skeleton are composites of a multi-rhombomeric NC origin. Within these compound elements, however, the original neuraxial order of crest deployment from the hindbrain is strictly maintained. Moreover, single-rhombomere resolution enabled us to observe an underlying, highly constrained pattern of skeletomuscular connectivity, which precisely relates to the rhombomeric origin of the individual crest subpopulations: each remains coherent throughout ontogeny, forming the connective tissue of individual branchial and tongue muscles as well as their respective attachment sites on both the NC-derived visceral skeleton (viscerocranium) and the mesodermally derived cranial base (neurocranium). Thus, cranial muscle connective tissues derived from a specific rhombomeric level are always exclusively attached to skeletal regions of the same origin. This striking match between skeletal elements and the connective tissues of their attached muscles addresses a fundamental question of head patterning - how do cranial muscles become specifically localised onto homogeneous looking skeletal elements?

MATERIALS AND METHODS

Rhombomere transplantations

Single rhombomeres were grafted isotopically and isochronically from quail to chick prior to neural crest emigration at HH stages 8+(5 somites) to 9+/10– (8-9 somites), depending on the axial level of the graft. Quail (*Coturnix coturnix japonica*) and Rhode Island Red hen's eggs from commercial sources were incubated at 37°C in a humidified atmosphere to HH stages 8+ to 9+. Quail donor embryos were removed from eggs, pinned out on a sylgard-coated dish in Howard's Ringer. Whole single rhombomeres with very small flaps of adjacent ectoderm were dissected out using flame-sharpened tungsten needles (100 μm wire) and unilaterally marked for later orientation with fine glass tips carrying 1% Nile Blue (Serva) in 2% agarose. For rhombomeres 3-7 visible boundary constrictions were used as landmarks for microsurgery. As crest emigration from r1 and r2 precedes r1/2 boundary formation, the presumptive r1/2 territory in st 8+/9– embryos was determined as follows. The future r2/3 boundary was estimated by counting 5 presumptive rhombomere lengths (90 μm each) from the level of the first somite (adjacent presumptive r7) to the front using an ocular micrometer. The neuroepithelial r1+2 territory delimited by this presumptive r2/3 boundary and the already visible mid-/hindbrain boundary was then bisected into pieces of equal rostrocaudal length (presumptive r1 and r2, respectively). For the grafts of midbrain NC at stage 8+ a 150 μm long piece of neuroepithelium in front of the mid-/hindbrain boundary was excised. To exclude mesodermal contamination, rhombomeres were carefully cleaned from adherent cells after treatment with dispase I (Boehringer-Mannheim, 1 mg/ml in L-15 medium; Gibco) for 20 minutes at room temperature, then washed and transplanted isotopically into exactly stage-matched chick hosts. To prepare hosts, the eggs were windowed and the embryos visualised by a small sub-blastodermal injection of India ink (Pelican yellow) made with a fine glass mouth pipette. A small hole was made through the vitelline membrane lateral to the site of operation and a single host rhombomere corresponding to the graft was excised with needles, leaving the notochord and pharyngeal endoderm intact. We used the same procedure and landmarks to determine rhombomeric positions in the host as described above for the donor. The quail graft was manoeuvred into place, with correct rostrocaudal orientation as determined by unilateral Nile Blue staining. The accuracy of this grafting procedure is documented in Fig. 1C-G. After moistening, the egg was sealed with electrical tape and reincubated for 3 hours. Operated embryos were then inspected and if the graft had not healed in properly, they were discarded. The chimeras were killed at E10, when the head is fully patterned (Tonkoff, 1900; McClearn and Noden, 1988), their heads fixed in Serra's fixative (ethanol 100%:formalin 37%:acetic acid, 6:3:1) overnight, dehydrated and embedded in Paraplast.

Assay and analysis of chimeras

364 operations were performed, 63 embryos obtained at E10 (viability 21%) and 42 chimeras at HH stages 13-19 (viability 70%). Each chimeric E10 head was paraffin wax embedded and cut into 10 μm horizontal sections. To detect quail nuclei, the majority of sections were processed with the quail-specific Q¢PN antibody (Developmental Studies Hybridoma Bank, University of Iowa), diluted 1:50, overnight. A peroxidase-conjugated goat anti-mouse IgG secondary antibody (Jackson) was used at 1:250 dilution for 1 hour, DAB staining performed for 20 minutes, endogenous peroxidase activity being blocked with 0.1% H_2O_2 in PBS and non-specific binding prevented with 5% FCS. To investigate early phases of crest migration and to test whether the chick-quail chimera technique yields the same results as previously obtained by focal DiI labelling of NC (Lumsden et al., 1991), 42 chimeras were harvested at HH st 13-19, fixed overnight in 3.5% paraformaldehyde and processed as wholemounts with the Q¢PN antibody (for 5 days at 4°C), all solutions containing 1% Triton X-100 (Sigma) to make tissues more permeable. Fig. 1C-G show that the NC migration pathways and locations in st 14-19 embryos are identical to those reported by Lumsden et al. (1991; cf. their Fig. 1). These controls gave us reason to believe that the chimera technique is also valid at later stages of development. Any possible delays due to embryonic healing thus appear negligible and do not systematically affect NC migratory pathways. Whole-mounts and sections were viewed on a Zeiss Axiophot with Nomarski optics allowing unequivocal identification of brown quail cells, cartilage, bone, muscle and connective tissues without couterstaining. Some sections were processed with standard Lison's hematoxylin nuclear stain (Lison, 1954; Couly et al., 1993), which shows quail nucleoli in black, cartilage in blue and bone in red. All chimeras were then

subjected to a rigorous screen for morphological abnormalities. Those whose skeletal or muscular elements showed any deformations/displacements or whose peripheral cranial nerve courses were aberrant were excluded from further analysis. After this preselection, 46 embryos were left, 38 of which were single rhombomere grafts (Table 1) and 8 were rhombomere-pair grafts (posterior midbrain+r1, *n*=1; r1+2, *n*=1; r2+3, *n*=3; r4+5, *n*=3). The latter grafts were made as additional controls in order to assess how the surgical procedure in single rhombomere grafts might disturb the rhombomeric interactions responsible for NC apoptosis over r3 and r5 (Graham et al., 1993), thus creating excess crest deployment from odd-numbered rhombomeres. If this had been the case, we would have found the added skeletal territories occupied by crest from single r2- and r3 grafts being more widespread than that occupied by crest from r2+3 in rhombomere-pair grafts. This was not observed (data not shown) and convinced us that additional crest production from r3 and r5 due to surgical artifacts was negligible.

As the grafts were bilateral, we assayed all 46 heads on both body sides for the presence of quail NC cells in 65 locations of the skeleton (braincase, visceral skeleton) and of all branchial and hypoglossal muscle connective tissues. When crest cells were present in a specific location in 80% of all embryos examined, we charted this location as being crest-derived from the specific origin. Its extent was superimposed in colour-coding onto camera lucida drawings of chick heads using Adobe Photoshop, as shown below. The camera lucida template drawings of cleared E10 chick heads stained for cartilage/bone with Alcian Blue/Alizarin Red were performed with ink on tracing paper and then scanned in. The skeletal nomenclature was adopted from Jollie (1957) and Baumel (1979) and that of the musculature from Barnikol (1952), Mc Clearn and Noden (1988), Kallius (1905) and Zweers (1974).

Table 1. Number of chimeras analysed

Type of isotopic graft	HH stage of operation	Beginning of crest emigration*	Number of chimeras analysed at	
			E10	st 13-19
caudal 150 μm of midbrain	8+	9	3	5
r1	8+	9+/10	5	7
r2	9–	9+/10	5	7
r3	9(+)	10+	5	6
r4	9(+)	10+	5	6
r5	9+	10+	4	6
r6	9+/10–	10+	5	5
r7	10–	10+	6	

*Data from Tosney (1982) as judged by timing of basal lamina fragmentation and changed ECM properties above emerging CNC populations.

RESULTS

Rhombomeric organisation of the avian jaw apparatus

The aim of this study was to determine the contribution made by the neural crest of each rhombomere to the avian jaw and tongue apparatus.

The avian jaw comprises a complex pattern of upper and lower elements, which are linked together and to the brain capsule (neurocranium) by joints and branchial muscles. The main upper jaw element is the pterygoquadrate, which has four articulations with surrounding elements: to the palatine bone (the roof of the palate) anteriorly, to the otic region (squamosal) posteriorly, to the quadratojugal/jugal bone laterally and to the lower jaw ventrally (Figs 1B, 2). The lower jaw skeleton in the embryo is composed of Meckel's cartilage, covered by several dermal bones (dentary, splenial, surangular, angular, gonial); the proximal end of Meckel's cartilage, forming the jaw joint, later ossifies endochondrally as the articular. The articular bone has two processes which serve as muscle attachment sites: the M.pterygoideus (N.V.) inserts onto the medially located internal process and the

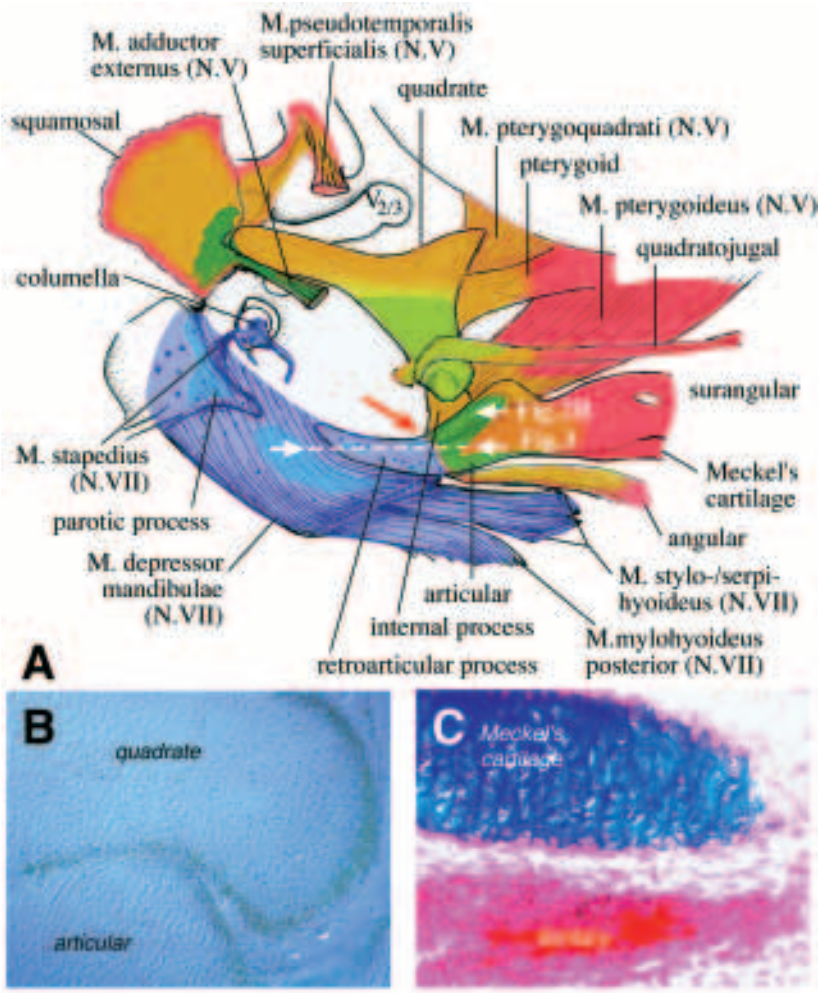

Fig. 2. (A) Lateral aspect of the otic region at E10. Colour coding as in Fig. 1A. Red arrow demarcates the invisible boundary between 1st and 2nd arch neural crest within the articular region of the lower jaw. Note the branchial arch specific (=colour) matching of muscle connective tissues and their respective skeletal jaw attachment sites. (B) Horizontal section through the quadratoarticular joint of an E10 r1 crest chimera (grafted at st 8+). In the mandibular arch skeleton rhombomeric crest (from r1+2) is restricted to proximal parts such as articular and quadrate surrounding the jaw joints. (C) Horizontal section through distal jaw region of a chimera in which the caudal 150 μm of midbrain/crest were isotopically replaced at st 8+. Only midbrain crest forms the distal part of the jaw, ie. Meckel's cartilage and dentary. In C cartilage is blue, bone is red and quail nuclei are black.

M.depressor mandibulae (N.VII) onto the retroarticular process. This prominent hyoid arch jaw-opening muscle connects the lower jaw to the otic capsule of the neurocranium (Fig. 2A).

We find that the fully patterned jaw apparatus is derived from neural crest cells, as have previous workers (Le Lièvre, 1974; Noden, 1978; Couly et al., 1993). Surprisingly, we also find that the jaw is composed of both mandibular and hyoid arch neural crest cells (Noden, 1983a; Figs 1B, 2). The skeletal area occupied by mandibular arch crest displays a subtle internal regionalisation, as individual crest populations (from posterior midbrain, r1 and r2) are differentially localised within it. In the articular region, this mandibular crest territory directly abuts onto a skeletal territory derived from hyoid arch NC (of r4, and to minor degrees r3 and r5). Although mandibular arch cells do not mix with hyoid arch cells, they collaborate in the formation of a lower jaw which displays no anatomical discontinuity.

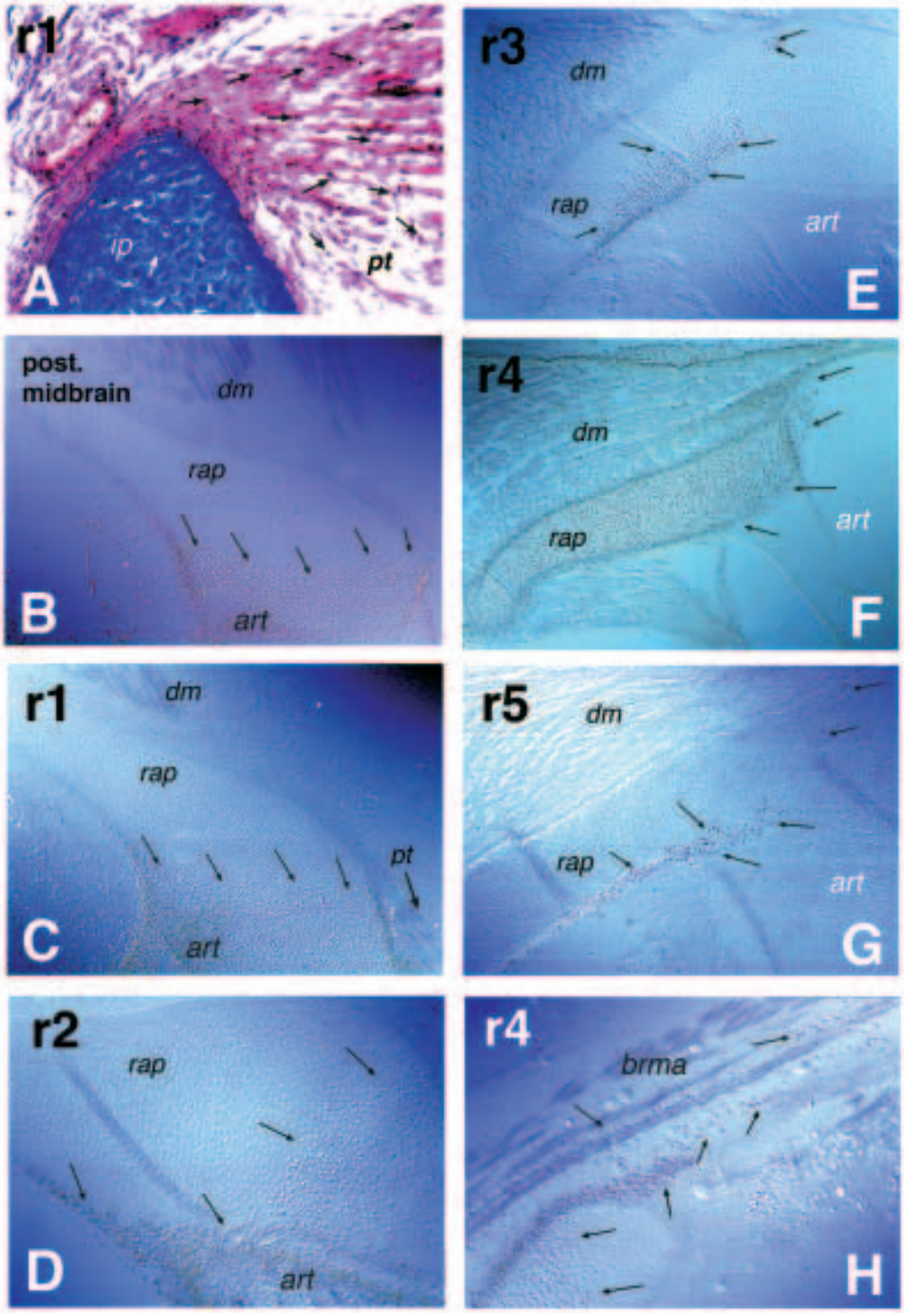

Fig. 3. Complementary and non-overlapping contribution of mandibular and hyoid crest to the avian lower jaw at E10, plane of horizontal sections is shown in Fig. 2. Cryptic boundary between different branchial arch populations is indicated by fine arrows. Mandibular crest from posterior midbrain and r1 (A-D) forms the articular (art) attachment regions of 1st arch muscles, as, for example, the internal process (ip) for the M. pterygoideus (pt, N.V; its CT, black arrows in A, is of the same origin). Complementary to and non-overlapping with the mandibular crest, the hyoid crest (from r4, 3 and 5) forms the retroarticular process (rap), which is the exclusive jaw attachment region of the M. depressor mandibulae (dm, N.VII; E-G) and M. branchiomandibularis (brma, N.IX, H). Note the small contributions of crest from r3 and r5 (E,G) within the strict confines of the mainly r4-derived skeletal domain (F).

Underlying combinatorial composition of the mandibular arch skeleton

The crest populations emanating from posterior midbrain, r1 and r2 occupy the adult mandibular arch skeletal territory in an overlapping, combinatorial manner. Distal elements, such as the upper jaw bones (maxilla, palatine, jugal), the major part of Meckel's cartilage and its overlying dermal bones (dentary, splenial), are derived solely from midbrain crest (Fig. 1D, pink in Fig. 1B), whereas the more proximal elements, centered around the jaw joint and close to the middle ear (articular, angular, surangular, quadrate, quadratojugal), are formed mainly by crest from r1 and 2 (Fig. 2B; yellow, green in Fig. 2A; cf. Noden, 1978). In the upper jaw, r1-derived NC is found throughout the pterygoquadrate, whereas midbrain crest is found only at its dorsal margin and articulations (orange in Fig. 2A) and r2 crest (green) where it preferentially surrounds the ventral articulations with lower jaw and quadratojugal. Although the boundaries between these individual crest populations are not absolutely sharp throughout the mandibular arch crest territory, cells from r1 and r2 were never found rostral to the rear quarter of the lower jaw.

Mandibular and hyoid arch crest cooperate in the formation of the jaw skeleton

While the crest from the midbrain and r1+ r2 merge into each other we find no mixing between these mandibular populations and those from the crest derived from r4 (+r3,r5). The quail marker reveals a distinct border between the mandibular arch crest populations (Fig. 3A-D) and the hyoid arch r4 (+r3, r5) crest population (Fig. 3E-H). This sharp demarcation between mandibular and hyoid crest populations (red arrow in Fig. 2A) does not coincide with any anatomical separation between skeletal elements, but traverses the articular region internally. Furthermore, this cryptic border separates the mandibular crest-derived insertion regions of all trigeminal (N.V) muscles from the hyoid crest-derived insertion region of facial (N.VII) muscles. The latter attach exclusively to the retroarticular process which is formed solely by hyoid crest from r4 (and to a smaller degree r3, r5) in all chimeras examined (Fig. 3E-G). The spatial extent of hyoid crest in the retroarticular process is exactly complementary to and non-overlapping with that of mandibular crest (compare arrows in Fig. 3A-D with those in 3E-H).

Crest from r3 was confined to a small contribution to the V2/3 and VII ganglia, the Schwann cell sheaths of the peripheral trigeminal (V2/3) and facial (VII) nerve branches and the hyoid skeletal elements (retroarticular process and columella, Figs 3E, 7E,F). In the latter case, r3 crest is always localised in small scattered areas within the precisely demarcated confines of r4 crest (Fig. 3E) and is always excluded from the mandibular crest territory. Similarly, the even smaller r5 crest population is also restricted to the r4 territory (Fig. 3G) and peripheral nerve sheaths of Nn.VI, VII and IX. We could not reliably detect r5 crest in any skeletal territory occupied by crest from r6 or r7 (3rd and 4th arch, although some scattered cells were seen in 3/16 skeletal locations examined.

The hyoid arch crest also forms the columella (avian homologue of the mammalian stapes, col, Fig. 7E,F), although its footplate was never entirely quail positive in our chimeras. Therefore we cannot exclude an ancillary contribution from the paraxial mesoderm forming the otic capsule (cf. Noden, 1983a; Couly et al., 1993).

Internal zonation of the tongue skeleton

The avian tongue skeleton consists of six elements: the paired paraglossals, the median basihyoid, the urohyal and the paired epi-/ceratobranchials (Fig. 4). A large number of hypoglossal (N.XII) and branchial muscles are inserted onto these elements in a highly specific configuration. Crest cells from all rhombomeric levels contribute to these elements, again in a highly ordered manner. Sharply defined borders between different NC populations do not coincide with anatomical features or gaps between elements (arrows in Fig. 5). An internal zonation of the tongue elements was observed in which mandibular arch crest from midbrain and r1 forms the major part of the paraglossals (pglo) and the anteroventral part of the basihyoid (vbhy, Fig. 5A-C). Non-overlapping with the mandibular crest, hyoid crest from r4 (containing small islands of r3 + r5 crest) constitute the posterior ends of the paraglossals and a more posterodorsal zone of the basihyoid (Fig. 5D-G). Crest from r6 and r7 (3rd and 4th branchial arch) forms the posterior roof of the basihyoid (dbhy, Fig. 5H) and the entire urohyal and epi-/ceratobranchials (uroh, epibr, cerbr, Fig. 5J,K). The common anterior boundary of crest from both r6 and r7 is complementary to and non-overlapping with that of the hyoid crest population (cf. arrows in Fig. 5J and G). In the epi-/ceratobranchials (epibr, cerbr), the r6 and r7 populations mix completely (Fig. 5J,K), whereas in the urohyal (uroh), r7 crest is localised throughout and r6 crest is confined more anteriorly. However, no boundary between these two populations is as distinct as their common border with the hyoid crest population.

As was found for the jaw skeleton, this zonal organisation

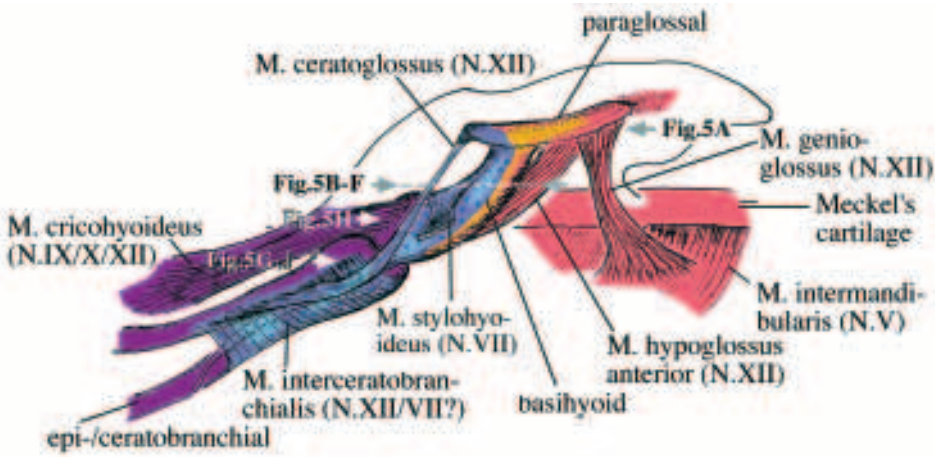

Fig. 4. Lateral view of the avian tongue skeleton and its associated branchial and tongue (hypoglossal) muscles. Note the internal zonation of the basihyoid and the branchial arch specific (=colour) matching of muscle connective tissues and their respective skeletal attachment regions.

respects the axial order of crest deployment from the embryonic hindbrain: mandibular arch crest lies anteroventral to hyoid crest as the latter does towards 3rd/4th branchial arch crest. Crest cells from all axial (branchial arch) levels join to form the apparently uniform composite elements of the tongue, where anatomical borders do not coincide with crest population boundaries. But, as will be shown below, these underlying invisible boundaries between individual crest populations delimit insertion sites of hypoglossal and branchial muscles on the homogeneous skeletal elements.

Specific cranial NC populations anchor all branchial muscles to the braincase

We found previously unreported focal clusters of cranial NC cells within the mesodermal-derived basal braincase (neurocranium) precisely at the places where branchial muscles are attached (Fig. 6). Moreover, these crest cells always belonged to the same rhombomeric population as the connective tissue (CT) fasciae of the respective muscles. We observed this specificity in all chimeras for all branchial muscles that are directly connected to the neurocranium. Varying combinations of crest

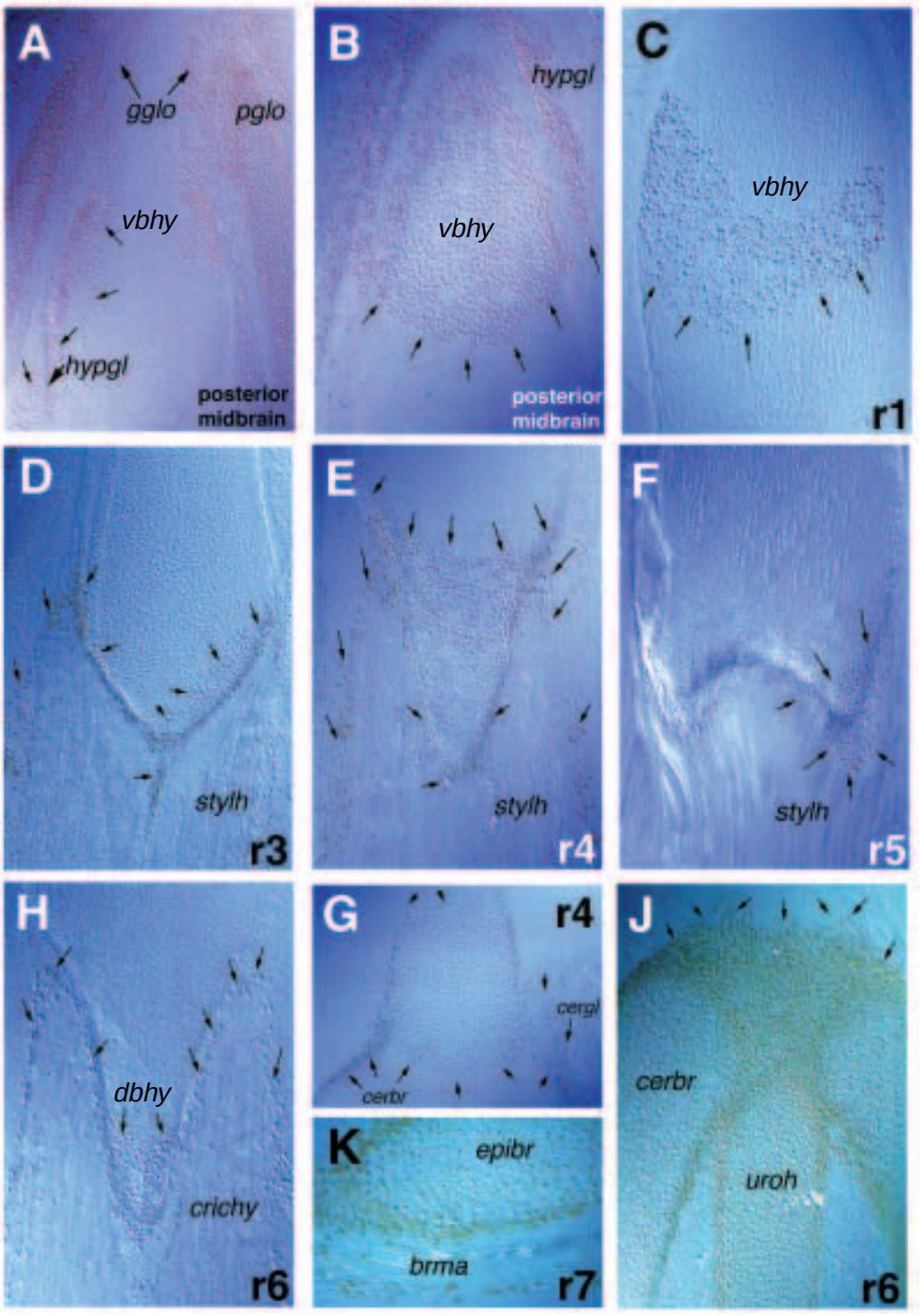

Fig. 5. Horizontal sections through the basihyoid in different rhombomeric chimeras reveal its internal zonation, plane of sections delineated in Fig.4. Mandibular arch crest from posterior midbrain forms the connective tissues of M. genioglossus (gglo, N.XII) and hypoglossus (hypgl, N.XII) and their respective attachment regions of the paraglossals (pglo) and ventral basihyoid (vbhy). Extent of 1st arch crest is complementary to that of 2nd arch crest from r4, 3 and 5. Note again the restriction of crest from r3 and 5 to the territory occupied by r4 crest. 2nd arch-derived skeletal territory is the exclusive tongue attachment region of M. stylohyoideus (stylh, N.VII, D, E, F) and M. ceratoglossus (cergl, N.XII, G). (H) Crest from r6,7 forms the most dorsal basihyoid (dbhy), epi-/ceratobranchial (epibr, cerbr), urohyal (uroh) and attached CTs of M. branchiomandibularis (brma, N.IX/X.) and cricohyoideus (crichy, N.IX/X/XII). Note sharp intraskeletal interface with hyoid crest (cf. arrows, G and J).

populations from posterior midbrain, r1 and r2 form the connective tissues and respective attachment sites of mandibular arch muscles (Fig. 7A-D), whereas crest predominantly from r4 does so for the hyoid arch muscles (Fig. 7H,J,K). Fig. 7A,B shows r1-derived quail NC chondrocytes (white arrows) inserted into the neurocranial wall. They are in direct continuity with connective tissue crest cells (black arrows) of the same axial origin, that anchor mandibular arch muscles (M. pseudotemporalis superfic.; mps in 7A and M. protractor pterygoquadrati; mprp in 7B) to these regions. Fig. 7C shows the same relationship for another mandibular muscle (M. adductor externus; mae, N.V) which is linked to the squamosal bone (sq), again by an NC-derived fascia of the same origin (r1+2) as this neurocranial bone (Fig. 7D detail). Interestingly, the squamosal bone sits on a small chondrocranial region (tegmen tympani; tty) of the same origin (Fig. 7C, arrows in cartilage) that is surrounded by quail-negative (mesodermal) prootic cartilage.

The ontogenetic unity of attachment site and muscle CT was also seen for the 2nd arch (hyoid) muscles (M. depressor mandibulae (dm) and M. stapedius (mstap) in Fig. 7E-K). The otic attachment region (parotic process; parp) of the depressor mandibulae, the most prominent hyoid arch muscle, is mainly derived from r4 crest as is its CT (Figs 3F, 6, 7J). The same is true for the stapedial muscle, which connects the columella to the braincase (Fig. 7E,G). Crest from r3 and r5 contribute to a very small extent to these hyoid muscle attachment regions and CTs (Fig. 7H,K).

Some of the muscle attachment points shown above (Fig. 7A,B,G-K) are localised in skull regions that have previously been mapped as being of solely mesodermal origin (‘chordal skeleton’, see Couly et al., 1993: areas 2 and 13a in fig. 4B and area 10 in fig. 14). The neurocranial areas that are specialised as muscle attachment sites are characterised only by their discrete ontogenetic origins from the NC, as detected by the quail marker; no other anatomical landmarks reveal their distinctive origin within the continuous sheet of the basicranial wall. Furthermore, their extent within the otherwise mesodermal domain is restricted to the insertion areas of the associated muscles, as the arrows in Fig. 7J exemplify. Despite close inspection, we could not find any branchial muscle CT of a specific crest origin linked to a neurocranial region of a different neuraxial origin.

Specificity of muscle attachments in the visceral skeleton

What we saw for the neurocranial attachment points of branchial muscles also holds for their viscerocranial insertions: muscle connective tissue is always exclusively anchored to skeletal domains derived from the same initial crest population. A single rhombomeric/branchial arch population gives rise to skeletal domains of the viscerocranium, the neurocranium and the branchial muscle connective tissues linking them together. This strict organisation becomes veiled by the fact that the skeletal elements are compounds of a multiple branchial arch crest origin.

This axial specificity is best seen at interfaces between different branchial arch crest populations within the same skeletal element (Figs 2A, 3). In the articular region of the lower jaw, mandibular and hyoid arch crest populations directly contact each other but do not overlap. Close to their interface, mandibular arch muscles attach exclusively to the mandibular crest territory: the CT of the M. pterygoideus (pt, N.V; arrows in Fig. 3A,C), for example, is inserted onto the internal process (ip) of the articular, which is derived from the same posterior midbrain and r1 crest populations (orange in Fig. 2A). The nearby retroarticular process (rap) serves as the only lower jaw attachment region of the hyoid arch muscles, depressor mandibulae (dm, Figs 2A, 3), serpihyoideus, stylohyoideus and posterior mylohyoideus. The retroarticular process and the inserted muscle fasciae are derived from r4. We could not find any cross-attachment of a muscle fascia of one branchial arch origin onto a skeletal derivative of another origin in any of the chimeras examined.

To explore the general nature of this branchial arch-specific association, we examined in detail the configuration of all muscle attachments onto the tongue skeleton and found the same specificity: hypoglossal muscles (such as the genioglossus, gglo, and the anterior and lateral hypoglossus; hypgl – pink areas in Fig. 4), whose fasciae are midbrain crest derived, are exclusively inserted onto midbrain crest-derived basihyoid cartilage (vbhy, arrows in Fig. 5A,B). Muscles whose connective tissues derive from hyoid crest, such as the stylohyoideus (stylh, N.VII, Fig. 5D-F), serpihyoideus, interceratobranchialis (N.VII/XII) and ceratoglossus (cergl, N.XII, Fig. 5G), are attached exclusively to hyoid crest-derived skeletal domains

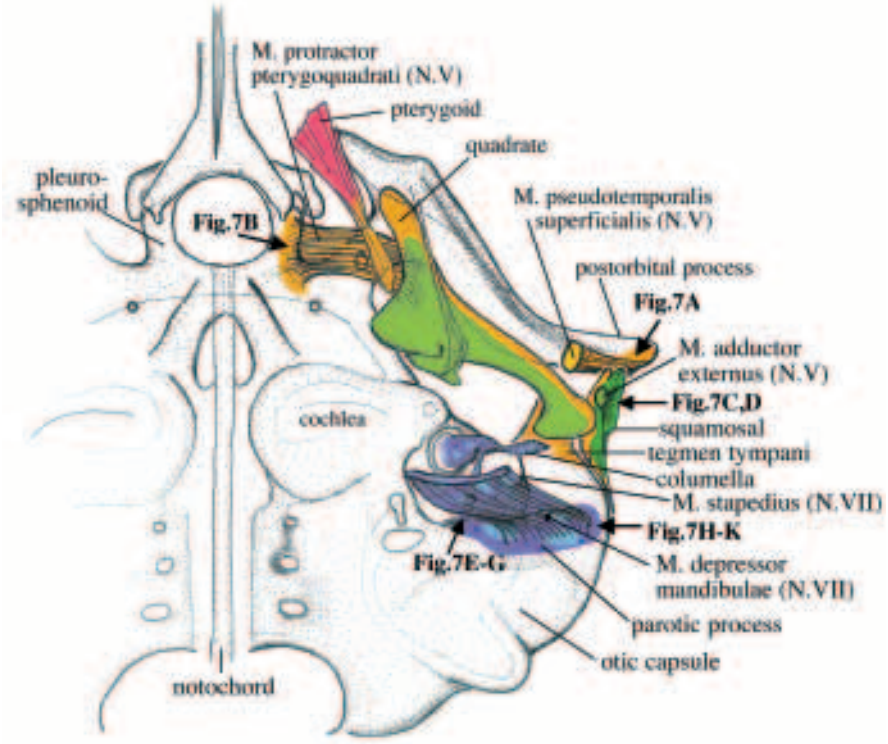

Fig. 6. Ventral view of the basicranium at E10 with attached branchial muscles. Colour coding as in Fig. 1A, arrows show the regions documented in Fig. 7.

(arrows). Similarly, muscles with fasciae derived from r6,7 crest such as the cricohyoideus (crichy, N.IX/X/XII, Fig. 5H) or branchiomandibularis (brma, N.IX, Fig. 5K, arrows) attach specifically to skeletal domains of the same axial origin. The branchiomandibularis muscle was the only muscle we could detect that derives its CT from more than one branchial arch. At its posterior end it is attached via r6+r7-derived CT to the epibranchial of the same origin (Fig. 5K), whereas at its anterior end it is attached to the hyoid crest-derived retroarticular process by hyoid crest-derived CT (Fig. 3H).

The entire pattern of cranial skeletomuscular connectivity is depicted in Fig. 9.

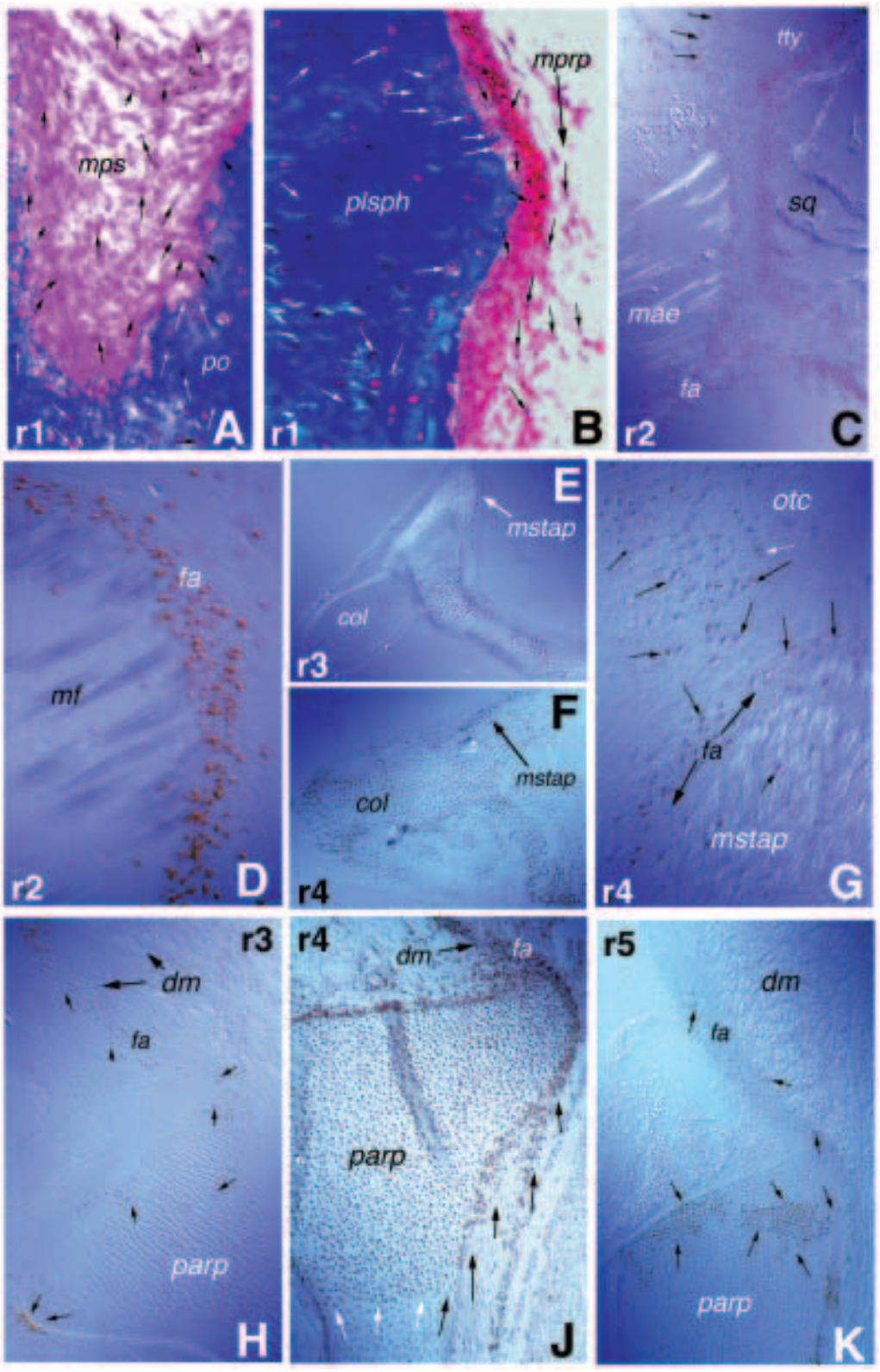

Fig. 7. Neurocranial anchor points of head muscles and their connective tissues are derived from the same distinct neural crest population. Focal clusters of r1-derived quail neural crest cells (white arrows) are inserted into the mesodermal basicranial wall, i.e. pleurosphenoid (plsph) and postorbital (po) cartilage region (blue in A,B). They are in direct contact with r1-derived CT cells (black arrows) of the attached muscles (M. pseudotemporalis superfic., mps; N.V in A, and M. protractor pterygoquadrati, mprp; N.V in B). (C) The squamosal bone (sq), is derived from r1+2 crest, sits on the otic capsule (tegmen tympani, tty, of the same origin, arrows) and is the attachment region of the M. adductor externus (mae, N.V), whose CT originates from crest of the same rostrocaudal neuraxial level. D shows that myofibrils (mf) of this muscle are quail negative and only the CT fasciae (fa) are crest derived. E,F show the 2nd arch-derived columella (col), which is connected to the cartilaginous otic capsule (otc; G) via the M. stapedius (mstap, N.VII). The CT fascia of this muscle (fa, arrows in E,G) as well as its focal cartilaginous attachment sites within the otic capsule and columella are again of the same axial neural crest origin. H,K show the small contribution of crest from r3 and 5 to the mainly r4-derived (J) otic attachment region (parotic process, parp) of the M. depressor mandibulae (dm, N.VII). White arrows in J indicate that the 2nd arch crest contribution to the otic capsule is confined to the attachment region of the associated muscle's fascia.

DISCUSSION

Composite architecture of the mandibular arch skeleton

Short survival fate mapping of NC populations emigrating from individual rhombomeres (Lumsden et al., 1991) has shown that the mandibular arch is colonised by crest from the midbrain, r1 and r2 (Fig. 1A). While crest from posterior midbrain and r1 are ubiquitously distributed within the mandibular arch territory, crest from r2 appears to be more restricted to its posterior margin close to the 1st branchial pouch. Long survival fate mapping using the quail marker has now allowed us to extend these observations; we have shown a specific combinatorial overlap of the respective populations in the fully patterned skeleton. We observed that distal elements, such as the major part of Meckel's cartilage, dentary, maxilla, and palatine bones are exclusively midbrain crest derived. Crest from r1 and r2 is restricted to proximal elements, such as the articular, pterygoquadrate and squamosal. The latter surround the middle ear cavity and form various articulations with each other and the adjacent neurocranium. These results are consistent with those of Noden (1978) who by grafting larger CNC domains found that 'metencephalic' neural crest occupies the more proximal skeletal parts of the 1st arch skeleton. This restricted proximal localisation of the hindbrain-derived mandibular crest is very interesting because it allows a more precise interpretation of the prominent craniofacial phenotypes associated with targeted mutations of *Hoxa-2* (Rijli et al., 1993; Gendron-Maguire et al., 1993) and *Otx-2* (Matsuo et al., 1995).

Only 1st arch crest was shown to be morphogenetically specified in terms of patterning (Hoerstadius and Sellman, 1946; Wagner, 1949; Noden, 1983a), however, it is devoid of any *Hox* gene expression. This might suggest that in fact it is the absence of *Hox* gene expression that is a prerequisite of morphogenetic specification and Hox genes would have different functions in the hindbrain and the emanating NC. Although *Hoxa-2* is expressed up to the r1/2 boundary in the hindbrain, it is independently regulated in the r2 crest and downregulated as the cells emerge (Prince and Lumsden, 1994). The most anterior *Hoxa-2* expressing NC cells populate the hyoid arch (Prince and Lumsden, 1994). If positional information is encoded by a specific combination of *Hox* gene expression (a '*Hox* code', Hunt et al., 1991) it might be expected that removal of *Hoxa-2* function would lead to respecification of second arch NC identity into that of first arch. Indeed, *Hoxa-2*$^{-/-}$ mice display a complete lack of 2nd arch structures and the formation, in their place, of certain 1st arch skeletal elements (Fig. 8). It was puzzling, however, that only the *proximal* mandibular elements such as malleus, incus, pterygoquadrate and squamosal were duplicated in the 2nd arch position, but not the distal elements (Meckel's cartilage, dentary, maxilla, palatine, jugal). In the light of Noden's conclusions (Noden, 1978, 1988) this phenotype was interpreted as either (a) the whole mandibular arch representing some kind of 'ground plan' default state of specification or, (b) a more specific transformation of 2nd arch identity into that of r1+2 crest (Rijli et al., 1993). Our fate map lends support to the second proposal of Rijli et al. (1993): based on established homologies between mammals and birds (Gaupp, 1912; Stadtmüller, 1936; Versluys, 1936; Allin, 1975; Maier, 1990), we find that precisely those elements that are derivatives of r1+2 crest (articular = malleus, quadrate = incus, pterygoquadrate, squamosal) are duplicated in the *Hoxa-2* knockout (dark green and asterisked in Fig. 8). Those of solely midbrain crest origin (distal Meckel's cartilage, dentary, maxilla, etc.) are not duplicated (red arrow in Fig. 8). This means that the *Hoxa-2* knockout did not create a general default 'ground pattern' of the mandibular arch skeleton in the 2nd arch location; rather, a more specific homeotic transformation might have occurred in which 2nd arch NC acquired the identity of rhombomeric 1st arch crest (from r1+2), but not midbrain crest. The *Hoxa-2/b-2* double knockout will show whether a more complete transformation can be achieved.

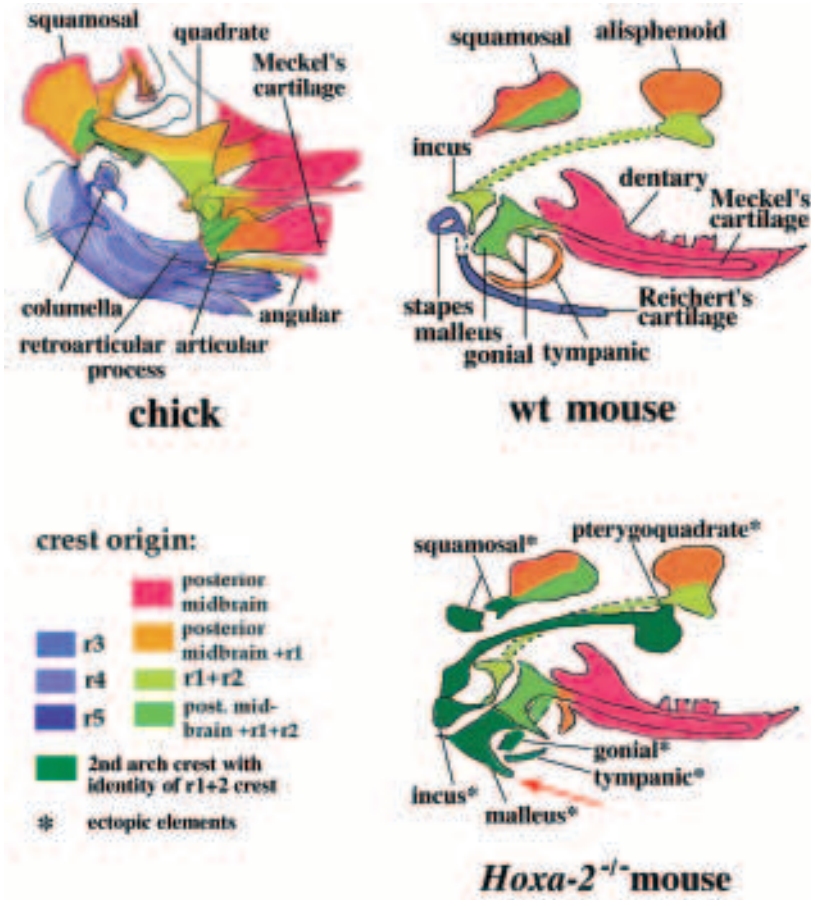

Fig. 8. Rhombomeric architecture of the avian and mammalian otic region as based on established homologies between sauropsids and mammals. Diagram contours of normal and mutant mouse heads after Rijli et al. (1993), colour coding superimposed according to the present study. In *Hoxa-2*$^{-/-}$ mice, 2nd arch crest identity (blue in wild type) is possibly homeotically transformed into that of crest from r1+2, as only elements normally containing r1 and 2 crest are duplicated in the 2nd arch location (dark green, ectopic elements marked with asterisks). Distal jaw elements (Meckel's cartilage, dentary etc) that are normally derived solely from midbrain crest (pink) are not duplicated in the mutant (red arrow).

Another very interesting, complementary craniofacial phenotype was found in the *Otx-2* heterozyzous mutants, where specifically the midbrain crest derivatives of the 1st arch are affected (Matsuo et al., 1995). *Otx-2* is normally expressed rostral to the mid-/hindbrain boundary and in the NC emigrating from the midbrain. In *Otx-2*$^{+/-}$ mice, the elements that we have mapped as being solely midbrain crest derived (distal Meckel's cartilage, dentary, maxilla, palatine) are lacking or severely reduced. The proximal, hindbrain-derived, 1st arch elements (malleus, incus, pterygoid) are almost unaffected. It is unknown whether this heterozygous phenotype results from the dose-dependent lack of *Otx-2* in midbrain crest cells or whether it is a secondary effect due to impaired specification of the (posterior) midbrain as a whole.

Our fate map and these distinct knockout phenotypes rather suggest that mandibular arch crest does not represent a simple 'default' state of morphogenetic specification, as stated by Noden (1978, 1983a) on the basis of heterotopic grafting experiments. On the contrary, the mandibular arch appears to be a complex patterning system in which crest cell populations of different states of maturation, axial origins and positional identities are differentially segregated and yet overlap in a combinatorial fashion. Notably, the multiple articulations between upper/lower jaw and neurocranium are confined to skeletal regions made by rhombomeric 1st arch crest. Heterotopic replacement of individual crest populations from midbrain, r1 and r2 will provide a test for the phenotypic predictions that can be made from our fate map as regards to the combinatorial patterning of the pterygoquadrate and the positioning of its joints.

In this context, the expression patterns of *Otx-2* and *proboscipedia* homologues (*Hoxa-2/b-2*) in the mandibular arch velar bars of the lamprey will be highly informative about the agnathan to gnathostome transition (Forey and Janvier, 1993; Maisey, 1994; Janvier, 1993). They will show whether downregulation of *Hoxa-2* within r2-derived NC is responsible for the acquisition of a pterygoquadrate and its various articulations. With the embryological framework provided by our fate map these genes might thus give us insight into the developmental evolution of the midbrain-hindbrain boundary and its significance for this fundamental morphological step in vertebrate history 500 million years ago: the evolution of jaws.

Developmental significance of NC from r3 and r5

Previous experiments have demonstrated that apoptotic depletion of crest cells in r3 and r5 (Graham et al., 1993) can account for the segmental generation of hindbrain NC (Lumsden et al., 1991) and is a result of interrhombomere interaction (Graham et al., 1993, 1994). Other studies using DiI labelling, videomicroscopy and short-term survival have shown that the dorsal region of r3 expands rostrocaudally during development and that small numbers of surviving crest cells from r3 concomitantly migrate within the neuroepithelium to exit on the level of r2 and r4 (Birgbauer et al., 1995). Thus, most r3 and r5 crest cells die and those that survive migrate from the hindbrain in a peculiar way; in the absence of a long term fate map, the developmental significance of these phenomena remained obscure. As might be expected for an interactive mechanism, crest depletion over r3, r5 is not absolute (Lumsden et al., 1991) and it is perhaps not surprising that there are survivors of r3 and r5 crest precursors (Sechrist et al., 1993): our fate map shows, however, that their contribution to the fully patterned head skeleton is small. They are restricted to islands of cells within the skeletal and muscle connective tissue derivatives of the 2nd branchial arch that are predominantly formed by crest from r4. To our surprise, the extent of crest from r3 and r5 precisely respected the sharp intraskeletal borders between hyoid and mandibular crest on one side and 3rd/4th arch crest on the other (Figs 3E,G, 5D,F,G,J). By contrast, NC from r6 and r7 mix freely with each other in their 3rd and 4th arch skeletal derivatives (Fig. 5G,J). This correlates well with the existence of NC apoptosis in r3 and 5 and its absence between r6 and 7 (Graham et al., 1993). This is consistent with the idea that the removal of r3 and r5 crest by apoptosis is a sculpting mechanism that ensures the segregation of the outflowing NC into discrete, segmental streams (Lumsden et al., 1991): the different crest populations that

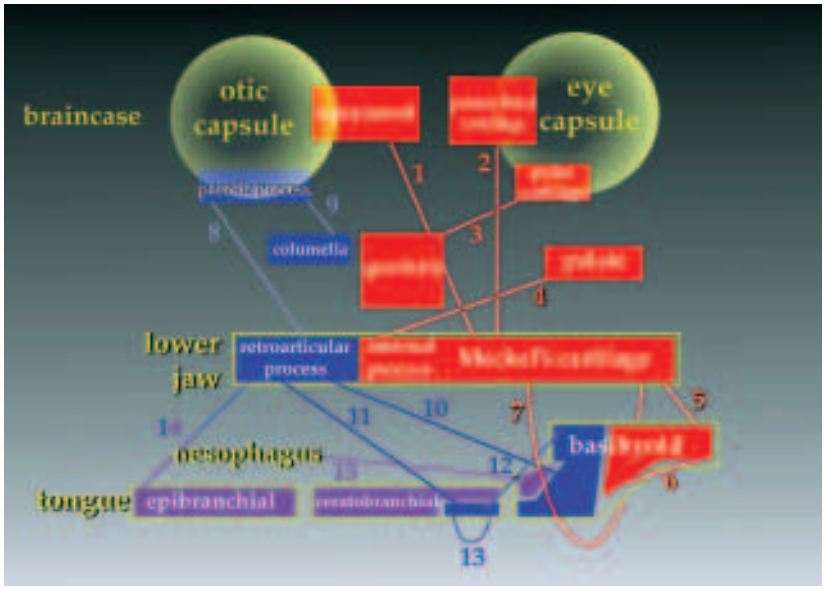

Fig. 9. Pattern of skeletomuscular connections in the avian head. Red depicts 1st arch, blue 2nd arch, purple 3rd/4rth arch neural crest derivatives. For details of individual elements compare Figs 1B, 2A, 4, 6. Lines represent mesenchymes of individual muscles. Each neural crest population remains coherent throughout ontogeny (proximodistal colour matching) and gives rise to muscle attachment regions on the braincase, the associated muscles' CTs and their respective viscerocranial attachment sites in compound skeletal elements (yellow boxes). 1, M. adductor externus, posterior, pseudotemporalis profundus (N.V). 2, M. pseudotemporalis superficialis (N.V). 3, M. protractor pterygoquadrati (N.V). 4, M. pterygoideus (N.V). 5, M. genioglossus (N.XII). 6, M. hypoglossus anterior and lateralis (N.XII). 7, M. intermandibularis (N.V). 8, M. depressor mandibulae (N.VII). 9, M. stapedius (N.VII). 10, M. stylohyoideus (N.VII). 11, M. serpihyoideus, mylohyoideus posterior (N.VII). 12, M. ceratoglossus (N.XII). 13, M. interceratobranchialis (N.XII/VII?). 14, M. branchimandibularis (N.IX/X). 15, M. cricohyoideus (N.IX/X/XII).

emigrate from even-numbered rhombomeres and colonize different branchial arches are kept apart during migration by crest-free spacing regions.

Compound nature of the visceral skeleton and its cryptic axial organisation

Individual elements of the visceral skeleton are composite structures derived from crest cells of multiple branchial arch origin. The boundaries between adjacent crest populations do not coincide with the borders of anatomical structures; rather, they span them as invisible interfaces. Noden (1983a) noted that the retroarticular process and the basihyoid are derived from 'myelencephalic' crest – although he claimed in an earlier paper (Noden, 1978) that the tongue skeleton is mandibular arch crest. These and other studies (Le Lièvre, 1974, 1978; LeLièvre and LeDouarin, 1975; Noden, 1983b, 1988) preceded the appreciation that segmentation is a fundamental feature of early hindbrain development (Lumsden and Keynes, 1989) which has consequences for the deployment of individual crest populations (Lumsden et al., 1991). Without reference to rhombomere boundaries as natural landmarks for transplantation, these previous studies neither required nor attempted the high spatial resolution provided by the present study. This can now clarify the contradictory issues raised by Noden's work (1978, 1983a,b).

We find that all of the branchial arches contribute to the tongue skeleton in a veiled, albeit highly organised manner: individual mandibular crest populations mix with each other in varying degrees but do not mix with crest colonising the hyoid arch, although both contribute to the lower jaw. This is not an artefact of selective, species-specific adhesive properties of quail versus chick cells: if it were, then we would have found clear segregation also between (e.g.) r1 and r2 populations.

Despite their heterogeneous axial origins, however, jaw and tongue are homogeneous in shape. They display a cryptic multilayered organisation which precisely maintains the initial axial order of crest deployment from the embryonic hindbrain: mandibular crest comes to lie rostral to hyoid crest and hyoid crest rostral to 3rd/4th branchial arch crest throughout ontogeny.

The compound nature of the visceral skeleton raises substantial objections to the idea that the whole pattern of branchial elements is encoded in individual crest populations prior to their emigration (Noden 1983a). The concept of premigratory crest specification was developed by Hörstadius and Sellman (1946), Wagner (1949) and Noden (1983a) on the basis of grafting experiments of mandibular arch only but not more posterior crest populations. The latter, however, are supposed to be the developmentally specified ones because they express varying combinations of *Hox* genes, whereas mandibular arch crest is devoid of any *Hox* gene expression. The anatomical homogeneity of branchial components suggests that other patterning mechanisms, spanning the whole rostrocaudal axis, act on different crest populations and recruit them into composite elements. By defining precisely the axial levels of the grafts, our fate map enables us to make predictions about the effect of whole rhombomere excisions and heterotopic crest replacements on these compound elements. These will conclusively answer the debated question of premigratory NC specification: whether it implies information on skeletal shapes or only on the rhombomere-specific pattern of skeletomuscular connectivity.

The compound nature of visceroskeletal elements has important functional consequences: it provides the mechanical basis for an integration of different branchial arch muscle activities. These are controlled by different rhombomere pairs (Lumsden and Keynes, 1989; Fortin et al., 1995) and often even work antagonistically on elements of a common insertion (Bock, 1964; Zweers, 1974). For example, the internal process and other mandibular crest-derived regions of the lower jaw serve as attachment sites for the jaw-closing adductor muscles, which are innervated by the trigeminal neurons of r2 and r3. Similarly, the hyoid crest-derived retroarticular process is the insertion site of the 2nd arch depressor mandibulae, which opens the jaw and which is innervated by facial motor neurons in r4 and r5. Even the branchiomandibularis, the 3rd arch muscle which acts as a tongue protractor, is inserted onto the retroarticular process via hyoid crest-derived connective tissue and attaches to the epibranchial cartilage via r6,7-derived connective tissue. Complex, often even antagonistic activities of such different muscles that are inserted onto common skeletal structures are of vital functional significance for a vertebrate. They require a highly constrained ontogenetic patterning mechanism which defines the precise location of every muscle insertion site onto the skeleton.

Specific crest populations anchor branchial muscles to the neuro- and viscerocranium

The most striking aspect of the underlying skeletomuscular organisation which we found, is the specificity with which muscles attach to skeletal domains of the same axial origin. This specificity is astonishing because these insertion sites on apparently uniform skeletal elements show no further anatomical specialisations that might distinguish them from each other, apart from their rhombomeric origin.

The triple contribution of single crest populations to the basal, mesoderm-derived neurocranium, muscle connective tissues and visceroskeletal insertions answers an old question of craniofacial pattern formation, which was rejuvenated by Noden (1986; McClearn and Noden, 1988): how do branchial muscles and hypoglossal muscles get anchored to specific regions within the homogeneous looking neuro- and viscerocranium? Do mesodermal and NC cells, which both contribute to the neurocranium, have different functions?

Distinct NC populations, as focally inserted muscular anchor points within the uniform mesodermal wall of the basicranium, indicate a specific function of crest versus paraxial head mesoderm in setting up skeletomuscular connectivity. Furthermore, our fate map discloses a highly specific pattern of skeletomuscular connections in which individual cranial NC populations remain coherent throughout ontogeny (Fig. 9); being veiled anatomically by the compound nature of the visceroskeletal elements, this underlying pattern could only be revealed at single rhombomere resolution. To our surprise, this same strict skeletomuscular specificity applies also to hypoglossal muscle attachment points. Previous mapping studies (Noden, 1983b; Couly et al., 1993) have shown that the myocytes and the innervation of these muscles are derived from the much more posterior axial levels of the first five somites. Their skeletal attachment fasciae, however, are derived from the more anterior axial levels of cranial NC.

As has been shown for the limb (Chevallier and Kieny, 1982) and also suggested for the head (Noden, 1983a, 1986), our study supports the view that the connective tissue is the patterning source for muscles, irrespective of the axial origin of their myoblasts. Furthermore, we show how the coherence of individual crest populations which ensheathe the paraxial head mesoderm (Noden, 1988) could implement the specific pattern of skeletomuscular connections; the crest populations seem to interact with adjacent embryonic tissues to create a common patterning system for the visceral and the tongue skeleton. Individual shapes of branchial elements would then be defined by other patterning mechanisms acting on the whole rostrocaudal and proximodistal axis, whereas precise skeletomuscular connectivity is defined by the axial origin of individual crest populations. Heterotopic transplantation of these individual crest populations respecting the axial levels as defined by our study are now required to test this supposition.

Coherence of rhombomeric NC populations throughout ontogeny

The persistent coherence of rhombomeric crest populations on the proximodistal axis and their strictly maintained order on the anteroposterior axis may have profound implications for the evolution of diverse head morphologies. These axial constraints would allow variation in the shapes of visceroskeletal elements without ever rendering them non-functional, because skeletal domains would always remain linked to the neurocranium via muscle connective tissue of the same axial origin. Such changes occurred, for instance, during the early evolution of mammals when the 2nd arch-derived retroarticular process and attached M. depressor mandibulae were lost and the M. stylohyoideus (N.VII) shifted its attachment point from the lower jaw (Fig. 2A) to the styloid process of the otic capsule (Gaupp, 1912; Allin, 1975).

Within the developmental framework of strictly maintained axial order, *Dlx* genes, for instance, which are differentially expressed on the proximodistal axes of the branchial arches, might play a role in proximodistal specification (Qiu et al., 1995). Molecular evolution of proximodistal branchial arch specifiers might then account for evolutionary transformations of viscerocranial and muscular structures and their relative positions with respect to the neurocranium: a scenario which is experimentally testable by misexpressing these genes on the proximodistal axis of the branchial arches.

Our fate map provides a reference for a detailed analysis of future gene-knockouts with specific craniofacial phenotypes and also for a wider comparative approach in other species. By focussing attention on individual rhombomeric crest populations as the ultimate basis of homology between their derivatives, such comparative studies will help to elucidate which molecular pathways have changed during evolution and that are thereby responsible for the fascinating diversity of vertebrate head structure.

We thank Anthony Graham and Ian McKay for carefully reading the manuscript and Per Ahlberg (BMNH, London) for stimulating discussions on early vertebrate head evolution. This work was supported by the Studienstiftung des Deutschen Volkes (FRG), the MRC and HHMI. G. K. is in receipt of a PhD studentship by UMDS Bursary and, previously, from the Studienstiftung des Deutschen Volkes. A. L. is an International Research Scholar of the HHMI.

REFERENCES

Allin, E. F. (1975). Evolution of the mammalian middle ear. *J. Morph.* **147**, 403-438.

Barnikol, A. (1952). Korrelationen in der Ausgestaltung der Schädelform bei Vögeln. *Morphol. Jahrb.* **92**, 373-414

Baumel, J. J. (1979). *Nomina anatomica avium*., New York: Academic Press.

Birgbauer, E., Sechrist, J., Bronner-Fraser, M. and Fraser, S. (1995). Rhombomeric origin and rostrocaudal reassortment of neural crest cells revealed by intravital microscopy. *Development* **121**, 935-945.

Bock, W. J. (1964). Kinetics of the avian skull. *J. Morph.* **114**, 1-42.

Chevallier, A. and Kieny, M. (1982). On the role of connective tissue in the patterning of the chick limb musculature. *Wilhelm Roux Arch. Dev. Biol.* **191**, 277-280.

Couly, G. F., Coltey, P. M. and Le Douarin, N. (1993). The triple origin of skull in higher vertebrates: a study in quail-chick chimeras. *Development* **117**, 409-429.

Forey, P. and Janvier, P. (1993). Agnathans and the origin of jawed vertebrates. *Nature* **361**, 129-134.

Fortin, G., Kato, F., Lumsden, A. and Champagnat, J. (1995). Rhythm generation in the segmented hindbrain of chick embryos. *J. Physiol.* **486.3**, 735-744.

Gans, C. and Northcutt, R. G. (1983). Neural crest and the origin of vertebrates: a new head. *Science* **220**, 268-273.

Gaupp, E. (1912). Die Reichertsche Theorie (Hammer-, Amboss- und Kieferfrage). *Arch. Anat. Entwickl. gesch.* **Jg. 1912 Supplement**, 1-416.

Gendron-Maguire, M., Mallo, M., Zhang, M. and Gridley, T. (1993). Hoxa-2 mutant mice exhibit homeotic transformation of skeletal elements derived from cranial neural crest. *Cell* **75**, 1317-1331.

Graham, A., Heyman, I. and Lumsden, A. (1993). Even-numbered rhombomeres control the apoptotic elimination of neural crest cells from odd-numbered rhombomeres in the chick hindbrain. *Development* **119**, 233-245.

Graham, A., Francis-West, P., Brickell, P. and Lumsden, A. (1994). The signalling molecule *Bmp-4* mediates apoptosis in the rhombencephalic neural crest. *Nature* **372**, 684-686.

Hörstadius, S. and Sellman, S. (1946). Experimentelle Untersuchungen über die Determination des knorpeligen Kopfskelettes bei Urodelen. *Nov. Act. Reg. Soc. Scient. Ups.* Ser. IV., **13**(8), 1-170.

Hunt, P., Giulisano, M., Cook, M., Sham, M.-H., Faiella, A., Wilkinson, D., Boncinelli, E. and Krumlauf, R. (1991). A distinct *Hox* code for the branchial region of the vertebrate head. *Nature* **353**, 861-864.

Janvier, P. (1993). Patterns of diversity in the skull of jawless fishes. In *The Skull* (ed. Hanken, J. and Hall, B.K.), Vol. 2, pp. 131-188. Chicago: University of Chicago Press.

Jollie, M. T. (1957). The head skeleton of the chicken and remarks on the anatomy of this region in other birds. *J. Morph.* **100**, 389-436.

Kallius, E. (1905). Beiträge zur Entwickelung der Zunge, II. Teil, Vögel, Anas. *Anat. Hefte*, 1. Abt., **28**, 308-579.

Le Douarin, N. (1969). Particularités du noyau interphasique chez la caille japonaise (Coturnix coturnix japonica). *Bull. Biol. Fr. Belg.* **103**, 435-452.

Le Lièvre, C. S. (1974). Rôle des cellules mésectodermiques issues des crêtes neurales céphaliques dans la formation des arcs branchiaux et du squelette viscéral. *J. Embryol. Exp. Morph.* **31**, 453-477.

Le Lièvre, C. S. (1978). Participation of neural crest-derived cells in the genesis of the skull in birds. *J. Embryol. Exp. Morph.* **47**, 17-37.

Le Lièvre, C. S. and Le Douarin, N. (1975). Mesenchymal derivatives of the neural crest: analysis of chimaeric quail and chick embryos. *J. Embryo. Exp. Morph.* **34**, 125-154.

Lison, L. (1954). Alcian blue G with chlorantine fast red 5B; a technique for selective staining of mucopolysaccharids. *Stain Techn.* **29**, 131-138.

Lumsden, A. and Keynes, R. (1989). Segmental patterns of neuronal development in the chick hindbrain. *Nature* **337**, 424-428.

Lumsden, A., Sprawson, N. and Graham, A. (1991). Segmental origin and migration of neural crest cells in the hindbrain region of the chick embryo. *Development* **113**, 1281-1291.

Maier, W. (1990). Phylogeny and ontogeny of mammalian middle ear structures. *Netherl. J. Zool.* **40** (1-2), 55-74.

Maisey, J. G. (1994). Gnathostomes (jawed vertebrates). In *Major Features Of Vertebrate Evolution, Short Courses In Palaeontology* **7**, pp. 1-56. A Publication of The Palaeontological Society.

Matsuo, I., Kuratani, S., Kimura, C., Takeda, N. and Aizawa, S. (1995) Mouse *Otx2* functions in the formation and patterning of rostral head. *Genes Dev.* **9**, 2646-2658.

Mc Clearn, D. and Noden, D. (1988). Ontogeny of architectural complexity in embryonic quail visceral arch muscles. *Am. J. Anat.* **183**, 277-293.

Noden, D. (1978). The control of avian cephalic neural crest cytodifferentiation, I. skeletal and connective tissues. *Dev. Biol.* **67**, 296-312.

Noden, D. (1983a). The role of the neural crest in patterning of avian cranial skeletal, connective and muscle tissues. *Dev. Biol.* **96**, 144-165.

Noden, D. (1983b). The embryonic origins of avian cephalic and cervical muscles and associated connective tissues. *Am. J. Anat.* **168**, 257-276.

Noden, D. (1986). Patterning of avian craniofacial muscles. *Dev. Biol.* **116**, 347-356.

Noden, D. (1988). Interactions and fates of avian craniofacial mesenchyme. *Development* **103 Supplement,** 121-140.

Prince, V. and Lumsden, A. (1994). Hoxa-2 expression in normal and transposed rhombomeres: independent regulation in the neural tube and neural crest. *Development* **120**, 911-923.

Qiu, M., Bulfone, A., Martinez, S., Meneses, J. J., Shimamura, K., Pedersen, R. and Rubenstein, J. L. R. (1995). Null mutation of Dlx-2 results in abnormal morphogenesis of proximal first and second branchial arch derivatrives and abnormal differentiation in the forebrain. *Genes Dev.* **9**, 2523-2538.

Rijli, F. M., Mark, M., Lakkaraju, S., Dierich, A., Dolle, P., and Chambon, P. (1993). A homeotic transformation is generated in the rostral branchial region of the head by disruption of Hoxa-2, which acts as a selector gene. *Cell* **75**, 1333-49.

Sechrist, J., Serbedzija, G. N., Scherson, T., Fraser, S.E. and Bronner-Fraser, M. (1993). Segmental migration of the hindbrain neural crest does not arise from its segmental generation. *Development* **118**, 691-703.

Stadtmüller, F. (1936). Kranium und Visceralskelett der Säugetiere. In *Handbuch der vergleichenden Anatomie der Wirbeltiere* (eds. L. Bolk, E. Göppert, E. Kallius, and W. Lubosch), Vol. 4, pp. 839-1016. Berlin: Urban und Schwarzenberg.

Tonkoff, W. (1900). Zur Entwicklungsgeschichte des Hühnerschädels. *Anat. Anz.* **18**, 297-304.

Tosney, K. W. (1982). The segregation and early migration of cranial neural crest cells in the avian embryo. *Dev. Biol.* **89**, 13-24.

Versluys, V. J. (1936). Kranium und Visceralskelett der Sauropsiden. In *Handbuch der vergleichenden Anatomie der Wirbeltiere* (eds. L. Bolk, E. Göppert, E. Kallius and W. Lubosch), Vol. 4, pp. 699-808. Berlin: Urban und Schwarzenberg.

Wagner, G. (1949). Die Bedeutung der Neuralleiste für die Kopfgestaltung der Amphibienlarven. *Rev. Suisse Zool.* **56**(33), 519-620.

Zweers, G.A. (1974). Structure, movement, and myography of the feeding apparatus of the mallard (*Anas platyrhynchos* L.) A study in functional anatomy. *Netherl. J. Zool.* **24**, 323-467.

(Accepted 4 July 1996)